JOURNAL OF AIRCRAFT
Vol. 30, No. 6, Nov.–Dec. 1993

Optimization of Aircraft Engine Suspension Systems

D. A. Swanson* and H. T. Wu†
Lord Corporation, Erie, Pennsylvania 16514
and
H. Ashrafiuon‡
Villanova University, Villanova, Pennsylvania 19085

An interactive computer program has been developed to design aircraft engine mounting systems used for vibration isolation. Mount design is largely driven by two competing criteria. Mounts must be soft enough to provide vibration isolation, yet stiff enough to support the engine without excessive motions. The constrained variable metric optimization technique is used to determine the mount design parameters which minimize the transmitted forces in the mounts, subject to constraints on the maximum allowable deflection of the engine to static forces. The design parameters are the stiffness and orientation of each individual engine mount. The aircraft engine is modeled as a rigid body that is mounted to a rigid base representing the nacelle. An example is used to show that the optimization technique is effective in designing engine mounting system.

Introduction

AIRCRAFT engine mounts have two main purposes: 1) to connect the engine and airframe together, and 2) to isolate the airframe from engine vibration. Vibratory forces are mainly caused by rotational unbalances in the engine, and result in increased stress levels in the nacelle, as well as high noise levels in the cabin. Recently, the increased utilization of more sophisticated and larger thrust engines has resulted in larger unbalance forces and more diversified operating conditions. This has increased the transmitted vibration, and challenged design engineers to create even more effective mounting system designs. One useful method for helping the design engineer to develop more effective mounting systems is through optimization techniques.

Previous studies on the optimization of engine mounting systems have focused mainly on automobile applications. Demic[1] optimized ride comfort and controllability of passenger vehicles by minimizing vertical and angular oscillations. In other studies, Bernard and Starkey[2] and Spiekermann et al.[3] attempted to reduce large transmitted forces by moving the system natural frequencies away from an undesired frequency range. In their simulation, the engine was modeled as a rigid body with six degrees of freedom (DOF), and the design parameters were the stiffness and orientation of each mount. To avoid a trivial solution where the natural frequencies of the system approach zero, an augmented function was formed where large design parameter changes were penalized. This technique can be successful in moving the natural frequencies of the system away from an input frequency. However, it does not necessarily minimize the transmitted forces in the mounts.

In the case of aircraft engine mounting systems, the design parameters are more complicated. Figures 1 and 2 show the installation configuration for a typical turboprop engine. The engine is attached to the aircraft structure (nacelle) by means of three elastomeric mounts. One left side mount can be seen in Fig. 1 between the engine and the nacelle (the tube-shaped structure). The bottom mount can be seen in Fig. 2 between the nacelle and gear box. The power of the engine is transmitted through the reduction gear box to the propeller. These components and their unbalance excitation operate at different frequencies. The rotational unbalances create dynamic force in the mounts which are directly transmitted to the airframe. Also, because the available space is very small, the motion of the engine must be limited within a certain envelope. This places a constraint on the maximum allowable deflection of the engine to static, or very low-frequency, forces. These low-frequency forces include the thrust and torque generated in the engine, as well as g-forces caused by aircraft maneuvers. The two design goals of minimizing the transmitted forces, and limiting the engine deflection to maximum allowable values, form the basis for the constrained optimization problem studied in this article. The problem is solved using a recursive quadratic programming technique based on a constrained variable metric approach.[4]

Equations of Motion

The equations of motion for the engine mounting system model are derived in this section. The engine is modeled as a rigid body with six DOF, which consist of a single translation and rotation around each of the X-Y-Z global coordinate axes.

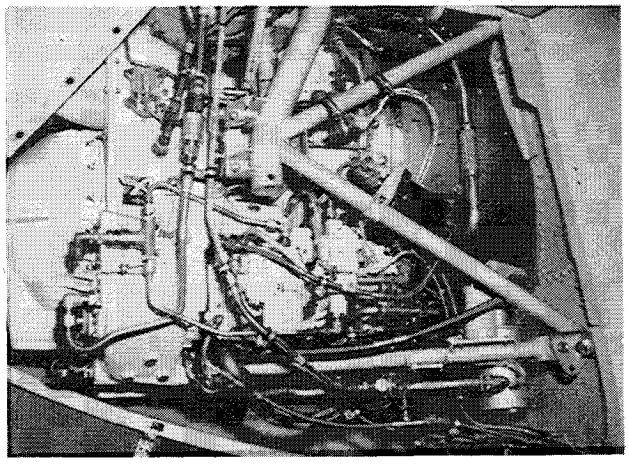

Fig. 1 Typical turboprop engine installation (port-side view).

Presented as Paper 91-1102 at the AIAA/ASME/ASCE/AHS/ASC 32nd Structures, Structural Dynamics, and Materials Conference, Baltimore, MD, April 8–10, 1991; received Sept. 4, 1991; revision received Aug. 13, 1992; accepted for publication Aug. 17, 1992.

*Engineer; currently Tomas Lord Research Center, Lord Corporation, Cary, North Carolina 27511. Member AIAA.
†Engineering Specialist, Aerospace Development, 1635 West 12th Street. Member AIAA.
‡Assistant Professor, Department of Mechanical Engineering.

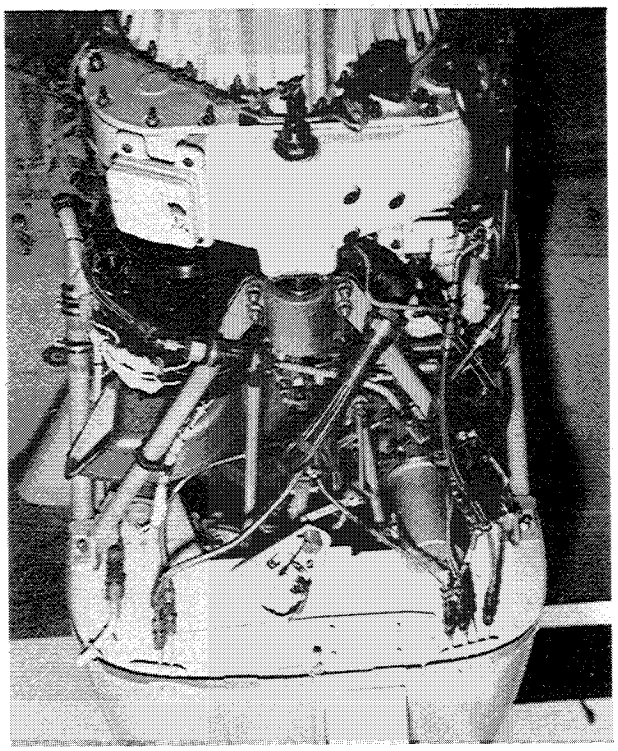

Fig. 2 Typical turboprop engine installation (bottom view).

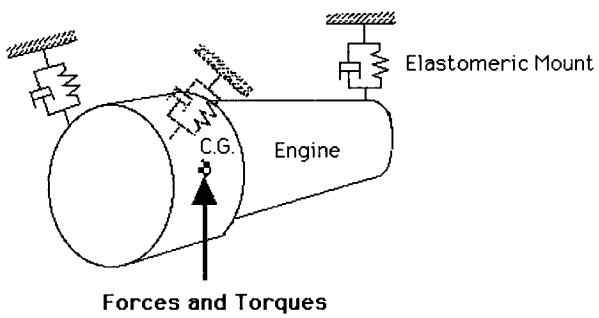

Fig. 3 Suspension system of an aircraft engine.

The engine is supported by an arbitrary number of mounts, which have arbitrary positions and orientations with respect to the engine center of gravity (c.g.), as shown in Fig. 3. The origin of the global coordinate system is located at the engine c.g.

The majority of mounts used in engine mounting applications are of a rubber bonded to metal, or elastomeric, construction. Elastomeric materials behave visco-elastically, and for this reason, a complex spring stiffness is used to model the dynamic behavior of the mount. The complex stiffness of a mount in the X, Y, and Z directions of its local coordinate system is defined by the equation

$$k^* = k' + jk'' = k'(1 + j\eta) \tag{1}$$

where k' and k'' are the resistive and dissipative spring rates, η is the loss factor, and $j = \sqrt{-1}$. No rational stiffness of the mounts will be considered. Another interesting characteristic of elastomeric mounts is that they generally possess a higher dynamic stiffness than static stiffness. To account for this, a dynamic-to-static spring ratio equal to k'/k is defined. A mount constructed from a purely elastic material will have a loss factor of zero, and a dynamic-to-static spring ratio of unity.

Based on Eq. (1), the stiffness matrix of an elastic, or viscoelastic, mounting in its local coordinate system can be written as

$$\bar{K}^* = \begin{bmatrix} k'_x + jk''_x & 0 & 0 \\ 0 & k'_y + jk''_y & 0 \\ 0 & 0 & k'_z + jk''_z \end{bmatrix} \tag{2}$$

This stiffness matrix must be transformed from the local mount coordinate system to the global coordinate system situated at the engine c.g. This is done through the following linear transformation:

$$K_i^* = A_i^T \bar{K}^* A_i \tag{3}$$

where A_i is the transformation matrix from the local coordinate system of the ith mount to the global coordinate system. The transformation matrix can easily be formed from the orientation of the mount with respect to the global coordinate system, which can be defined using Euler angles, Bryant angles, direction cosines, etc.[5]

To express the equations of motion in terms of the displacements and rotations at the engine c.g., another transformation is necessary. This transformation relates the displacement of each mount to the displacements and rotations of the engine c.g. Assuming that the engine displacements are small enough that they can be considered as infinitesimal displacements, the transformation of the engine displacements to the translational displacements at the mounting point i can be written as

$$\begin{aligned} \boldsymbol{u}_i &= \boldsymbol{U}_t + \boldsymbol{U}_r \times \boldsymbol{r}_i \\ &= \boldsymbol{U}_t - \boldsymbol{r}_i \times \boldsymbol{U}_r \end{aligned} \tag{4}$$

where $\boldsymbol{u}_i$ is the translational displacement vector at the mounting point i and $\boldsymbol{r}_i$ is the position vector of mount i with respect to the engine c.g. $\boldsymbol{U}_t$ and $\boldsymbol{U}_r$ are the respective translational and rotational displacement vectors of the engine c.g. In matrix form, Eq. (4) can be rewritten as

$$\boldsymbol{u}_i = (I - \tilde{r}_i) \begin{pmatrix} \boldsymbol{U}_t \\ \boldsymbol{U}_r \end{pmatrix} \tag{5}$$

where I is the (3 × 3) identity matrix, and $\tilde{r}_i$ is the (3 × 3) matrix defined for a vector cross product operation.[5] In terms of the mount displacement, the viscoelastic force vector $\boldsymbol{v}_i$ transmitted from mount i to the engine is

$$\boldsymbol{v}_i = -K_i^* \boldsymbol{u}_i = (-K_i^* K_i^* \tilde{r}_i) \begin{pmatrix} \boldsymbol{U}_t \\ \boldsymbol{U}_r \end{pmatrix} \tag{6}$$

where K_i^* is the dynamic complex stiffness matrix of mount i. The moment vector $\boldsymbol{t}_i$ that results from the application of the viscoelastic forces of mounting i on the engine c.g. is

$$\begin{aligned} \boldsymbol{t}_i &= -\boldsymbol{v}_i \times \boldsymbol{r}_i \\ &= \boldsymbol{r}_i \times \boldsymbol{v}_i \\ &= \tilde{r}_i \boldsymbol{v}_i \\ &= \tilde{r}_i^T K_i^* \boldsymbol{u}_i \\ &= (\tilde{r}_i^T K_i^* - \tilde{r}_i^T K_i^* \tilde{r}_i) \begin{bmatrix} \boldsymbol{U}_t \\ \boldsymbol{U}_r \end{bmatrix} \end{aligned} \tag{7}$$

Combining Eqs. (6) and (7) yields

$$\boldsymbol{e}_i = \begin{bmatrix} \boldsymbol{v}_i \\ \boldsymbol{t}_i \end{bmatrix} = \begin{bmatrix} -K_i^* & K_i^* \tilde{r}_i \\ \tilde{r}_i^T K_i^* & -\tilde{r}_i^T K_i^* \tilde{r}_i \end{bmatrix} \begin{bmatrix} \boldsymbol{U}_t \\ \boldsymbol{U}_r \end{bmatrix} \tag{8}$$

where e_i is defined as a generalized viscoelastic loading vector resulting for mount i that encompasses both forces and moments at the engine c.g. in all six DOF. By summing all of the viscoelastic loadings from a total of n mounts, the total viscoelastic loading vector on the engine c.g. can be expressed as

$$e = \sum_{i=1}^{n} e_i = \begin{bmatrix} -\sum_{i=1}^{n} K_i^* & \sum_{i=1}^{n} K_i^* \tilde{r}_i \\ \sum_{i=1}^{n} \tilde{r}_i^T K_i^* & -\sum_{i=1}^{n} \tilde{r}_i^T K_i^* \tilde{r}_i \end{bmatrix} \begin{bmatrix} U_t \\ U_r \end{bmatrix} \tag{9}$$

Next, we define $U = (U_t^T, U_r^T)^T$ as a generalized coordinate vector which represents the X, Y, and Z displacements and rotations of the engine c.g.

For elastic mounts possessing viscous damping, a viscous damping element is also included as an analysis option. Using a similar assembly procedure to the mount loading vector, the total damping loading vector on the engine c.g. resulting from a total of m dampers is

$$d = \sum_{i=1}^{m} d_i = \begin{bmatrix} -\sum_{i=1}^{m} D_i & \sum_{i=1}^{m} D_i \tilde{r}_i \\ \sum_{i=1}^{m} \tilde{r}_i^T D_i & -\sum_{i=1}^{m} \tilde{r}_i^T D_i \tilde{r}_i \end{bmatrix} \dot{U} \tag{10}$$

where D_i is the damping matrix of a viscous damper i. With all of the component reactive forces derived in terms of the generalized coordinates in Eqs. (9) and (10), the dynamic equations of motion for the engine can now be expressed using Newton's second law

$$M\ddot{U} = e + d + f \tag{11}$$

where M is the generalized mass matrix, d is the generalized damping force defined in Eq. (10), and e is the generalized mount force defined in Eq. (9). The vector f represents the external excitation force vector applied to the engine. Substituting Eqs. (9) and (10) into Eq. (11) results in

$$M\ddot{U} + D\dot{U} + (K' + jK'')U = f \tag{12}$$

$$D = \begin{bmatrix} \sum_{i=1}^{m} D_i & -\sum_{i=1}^{m} D_i \tilde{r}_i \\ -\sum_{i=1}^{m} \tilde{r}_i^T D_i & \sum_{i=1}^{m} \tilde{r}_i^T D_i \tilde{r}_i \end{bmatrix} \tag{13}$$

$$K' + jK'' = \begin{bmatrix} \sum_{i=1}^{n} K_i^* & -\sum_{i=1}^{n} K_i^* \tilde{r}_i \\ -\sum_{i=1}^{n} \tilde{r}_i^T K_i^* & \sum_{i=1}^{n} \tilde{r}_i^T K_i^* \tilde{r}_i \end{bmatrix} \tag{14}$$

$$M = \begin{bmatrix} m & 0 & 0 & 0 & 0 & 0 \\ 0 & m & 0 & 0 & 0 & 0 \\ 0 & 0 & m & 0 & 0 & 0 \\ 0 & 0 & 0 & I_{xx} & I_{xy} & I_{xz} \\ 0 & 0 & 0 & I_{xy} & I_{yy} & I_{yz} \\ 0 & 0 & 0 & I_{xz} & I_{yz} & I_{zz} \end{bmatrix} \tag{15}$$

where m is the mass of the engine, and Iij are the elements of the inertia tensor.

The static equilibrium equations of the engine can be developed by setting the velocity and acceleration terms in Eq. (12) equal to zero

$$K_{st} U_{st} = f_{st} \tag{16}$$

where K_{st} is the static stiffness matrix of the mounting system, and f_{st} is the generalized static loading.

Solution to the Equations of Motion

Two types of excitation are considered, low frequency or static forces and torques, and dynamic forces and torques.

Response to Static and Maneuvering Loads

The deflections of the engine c.g. to static and maneuvering conditions can be calculated from the solution of Eq. (16)

$$U_{st} = K_{st}^{-1} f_{st} \tag{17}$$

Four types of static and maneuvering excitation conditions exist, forces due to engine weight, reaction torques due to engine rotation, "g" forces due to aircraft maneuvers, and thrust forces due to the engine's thrust. The equivalent generalized static loading force at the engine c.g. for a weight force W applied at the engine c.g. is

$$f_{st} = \begin{bmatrix} W \cos \psi_{g1} \\ W \cos \psi_{g2} \\ W \cos \psi_{g3} \\ 0 \\ 0 \\ 0 \end{bmatrix} \tag{18}$$

where ψ_{g1}, ψ_{g2}, and ψ_{g3} are the direction cosine angles between the gravitational direction vector and the engine global coordinate system. The equivalent maneuvering force for a torque applied to the engine is

$$f_{st} = \begin{bmatrix} 0 \\ 0 \\ 0 \\ l \cos \psi_{11} \\ l \cos \psi_{12} \\ l \cos \psi_{13} \end{bmatrix} \tag{19}$$

where l is the magnitude of the torque, and the direction cosines of the torque with respect to the engine global coordinate system are equal to ψ_{11}, ψ_{12}, and ψ_{13}. For a constant thrust force f applied to the rigid body engine at location p, the generalized loading vector becomes

$$f_{st} = \begin{bmatrix} f \\ \tilde{p} f \end{bmatrix} \tag{20}$$

The equivalent maneuvering force for a constant acceleration excitation of "n" gees is

$$f_{st} = \begin{bmatrix} nW \cos \psi_{g1} \\ nW \cos \psi_{g2} \\ nW \cos \psi_{g3} \\ 0 \\ 0 \\ 0 \end{bmatrix} \tag{21}$$

Response to Dynamic Forces and Rotational Unbalances

The response of the engine c.g. to dynamic inputs can be calculated through the solution of Eq. (12). In the frequency domain, this can be found from the complex matrix inversion

$$U = [(K' - \omega^2 M) + j(\omega D + K'')]^{-1} f \tag{22}$$

The dynamic forces transmitted through the mount can then be calculated using Eq. (6). Two types of dynamic forces act on the engine: 1) rotational unbalances and 2) dynamic forces.

In the case of a rotational unbalance acting at a single frequency, the generalized dynamic force vector is

$$f = \begin{bmatrix} \sum_{j=1}^{p} f_j^* \\ \sum_{j=1}^{p} \tilde{t}_j f_j^* \end{bmatrix} e^{j\omega t} \tag{23}$$

where

$$f_j^* = \frac{T_j \omega^2}{g} \begin{bmatrix} \cos \varphi_{j1} \\ \cos \varphi_{j2} \\ \cos \varphi_{j3} \end{bmatrix} \tag{24}$$

where φ are the angles of rotary unbalance j with respect to the X, Y, and Z axes, $\tilde{p}_j$ is the position vector of the rotary unbalance j, T_j is the maximum amplitude of the rotary unbalance j, ω is the excitation frequency, and g is the gravitational constant.

In the case of force excitation, for k forces $f_1, f_2, \ldots, f_k$ having phase angles $\phi_1, \phi_2, \ldots, \phi_k$ with respect to some time reference and acting on the engine at locations $p_1, p_2, \ldots, p_k$; the total excitation is in the same form as in Eq. (23), except that

$$f_k^* = \begin{bmatrix} f_k^* \cos \varphi_{kx}(\cos \phi_k + j \sin \phi_k) \\ f_k \cos \varphi_{ky}(\cos \phi_k + j \sin \phi_k) \\ f_k \cos \varphi_{kz}(\cos \phi_k + j \sin \phi_k) \end{bmatrix} \tag{25}$$

Optimization

The optimization process consists of determining a set of elastomeric mount characteristics that minimize the transmitted forces through all of the mounts when the system is subjected to excitations of different amplitudes, phases, and frequencies. The optimal mounting system must also satisfy inequality constraints on the maximum allowable static deflection at the engine c.g., and/or some other critical locations.

Mathematically, the optimization problem can be expressed as

minimize

$$\Phi(X) \qquad X \in \mathrm{R}^n \tag{26}$$

subject to

$$C_k(X) \geq 0 \qquad k \in \mathrm{I}(1, \ldots, c) \tag{27}$$

where Φ is the objective function, X is a design parameter vector consisting of mount stiffnesses and/or orientations, $C_k(X)$ is a vector containing the inequality constraint equations, and c is the total number of constraints.

The objective function in Eq. (26) is related to the weighted sum of the magnitude of the transmitted dynamic forces, and encompasses the forces across all of the mounts in all directions, for all forcing conditions. Weighting factors are used to represent the importance of each forcing condition, mount number, and mount direction. The dynamic forcing conditions include cruise and takeoff, and can represent different forces at different frequencies and phases. The exact form of the objective function is

$$\Phi(X) = \sum_{i=1}^{ncond} S_i \sqrt{\sum_{j=1}^{nm} S_{xj}(f_{xij})^2 + S_{yj}(f_{yij})^2 + S_{zj}(f_{zij})^2} \tag{28}$$

where *ncond* is the number of excitations, nm is the number of mountings, S are the weighting factors, and f are the dynamic forces in each mount, in each direction, in the global coordinate system. The objective function weighting factors are user-defined numbers ranging from zero to one which specify the relative importance of each individual vibratory excitation, or force condition, in each direction of the global coordinate system (x, y, or z). These weighting factors are not unique, and different solutions will be obtained for different sets of weighting factors. Typically, the optimization procedure is initially run with all weighting factors equaling unity. If necessary, the procedure can be rerun with different sets of weighting factors. The constraint equations are of the form

$$C_i = |U_{st}|_i - (U_{max})_i \tag{29}$$

where C_i is the ith constraint equation, $|U_{st}|_i$ is the absolute value of the ith actual static deflection of the engine, and $(U_{max})_i$ is the ith maximum allowable static deflection of the engine. Since both the objective function and constraint equations are nonlinear, a nonlinear constrained optimization technique must be used to solve for the optimal solution. Constrained variable metric optimization technique[6] was used to solve the above optimal design problem.

Numerical Example

The configuration of a two-cylinder piston engine, with a utility engine located in between the two cylinders, is shown in Fig. 4. The engine weighs 1660 lb, and its mass moment of inertias are shown in Table 1. The c.g. of the engine, as well as the utility engine, is located at (0, 0, 0) of the global coordinate system. The c.g. of the two cylinders are located at (0, 1, 0) and (0, −1, 0), respectively. The original design of the suspension system consists of four identical axisymmetric mounts with static spring rates of $Kx = Ky = Kz = 8757$ lb/in. The dynamic-to-static spring rate ratio is 1.2, and the loss factor is 0.06. The location and orientation of each mount is listed in Tables 2 and 3, respectively. Bryant angles are used to represent the orientation of the mounts with respect to the global coordinate system. The design variables are the stiffnesses of the mounts, and these four mountings must be identical. It is also required that the mounts be axisymmetric, i.e., $K_y = K_z$ in the mount's local coordinate.

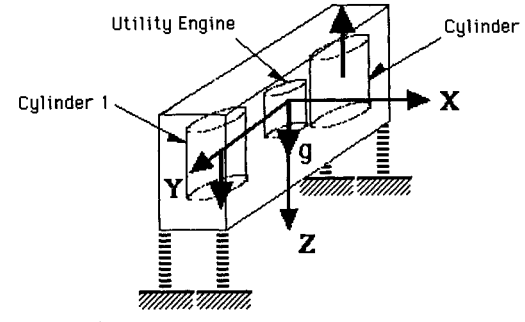

Fig. 4 Two-cylinder engine.

Table 1 Engine inertia, lb-in-s²

	X	Y	Z
X	216	0	207
Y	0	1293	0
Z	207	0	1285

Table 2 Mounting locations, in.

	X	Y	Z
c.g.	0	0	0
Mount 1	23.63	8.20	−11.79
Mount 2	23.63	−8.20	−11.79
Mount 3	−11.66	−8.20	−10.74
Mount 4	−11.66	8.20	−10.74

Two maneuvering conditions, along with the weight, are considered for the constraints on the maximum deflection of the engine subjected to low-frequency excitation. The first maneuvering condition is a "gee" force acting as the engine c.g. in the X direction. The second maneuver is a torque of 1000 in.-lb in the negative X direction. The maximum allowable deflections for these maneuvering conditions are

$$\begin{aligned} &|U_{tx}| \le 0.03, \quad |U_{ty}| \le 0.03, \quad |U_{tz}| \le 0.08 \quad \text{(in.)} \\ &|U_{rx}| \le 0.02, \quad |U_{ry}| \le 0.10, \quad |U_{rz}| \le 0.02 \quad \text{(rad)} \end{aligned} \tag{30}$$

Two engine cruise modes are considered for the minimization of the transmitted forces. In the first cruise mode, the engine is running at 40 Hz, while in the second cruise mode the engine is running at 80 Hz. The utility engine runs with the same frequency as the engine. Specific details of the two dynamic forcing conditions are listed in Tables 4 and 5. The weighting factor for the first dynamic forcing condition at 40 Hz is 0.5, while the weighting factor for the second dynamic forcing condition is 1.0.

Table 3 Mounting orientation, Bryant angles in degree

	θ_X	θ_Y	θ_Z
Mount 1	0	90	0
Mount 2	0	90	0
Mount 3	0	90	0
Mount 4	0	90	0

Table 4 Forcing condition of cruise mode 1

	Magnitude	Phase	Position	Direction cosine
Cylinder 1	1.0	0	(0, 1, 0)	(0, 0, 1)
Cylinder 2	1.0	0	(0, −1, 0)	(0, 0, −1)
Utility cylinder	0.5	0	(0, 0, 0)	(0, 0, 1)

Table 5 Forcing condition of cruise mode 2

	Magnitude	Phase	Position	Direction cosine
Cylinder 1	0.25	0	(0, 1, 0)	(0, 0, 1)
Cylinder 2	0.25	0	(0, −1, 0)	(0, 0, −1)
Utility cylinder	1.00	0	(0, 0, 0)	(0, 0, 1)

Table 6 Comparison between original and optimized systems

	Original system	Optimized system
Objective function	0.493	0.099
K_X, Axial stiffness	8,757	10,635
K_Y and K_Z, Radial stiffness	8,757	22,322
Natural frequencies, Hz	8.52	10.06
	11.11	12.99
	15.74	18.36
	16.21	25.55
	22.69	32.25
	39.94	60.38

The original design and corresponding optimal solution is shown in Table 6. From this table, it can be seen that the objective function of the optimized system is approximately one-fifth the objective function of the original system. One reason for this dramatic improvement is that one of the natural frequencies of the original system is 39.94, which is very close to an input forcing frequency of 40 Hz. The optimization successfully lowered the dynamic forces in the mounts by changing the mount stiffnesses. This resulted in a movement of the natural frequencies of the system away from the resonant condition at 40 Hz.

In any constrained optimization, it is important to see which constraints limit the performance of the system. These constraints are called active, or binding, and can be located where the static deflection equals its corresponding maximum allowable deflection value. Knowledge of the active constraints is important because only these constraints limit the system's performance. Small changes in the values of the maximum allowable deflection for the other constraints will have no effect on the optimal solution. The deflections of the optimized system at the engine c.g. are shown in Table 7. It can be seen that the rotation around the X axis in the second maneuvering condition is equal to its constraint value.

Because the objective function to be minimized is nonconvex, multiple local minima might be present. To see if multiple local minima were present for this problem, two other starting points, one with very soft mounts and one with very stiff mounts, were optimized. For the first starting point, each mount had an axial static stiffness of 4000, and a radial stiffness of 2000 lb/in. The initial and optimized systems for this soft starting point are shown in Table 8. Notice that the objective function for the optimized system is actually larger than that of the original system. The reason for this is that the starting stiffnesses are so soft that the static deflections at the engine c.g. violate the constraints in Eq. (30). This starting point is not feasible (it doesn't satisfy the constraints). The optimized system has the lowest value of the objective function that satisfies the constraints.

From Table 8, it can be seen that while the axial stiffness is almost identical as the first optimized axial stiffness, the optimal radial stiffness decreased dramatically from 22,322 to 2418 lb/in. Also, the optimized objective function is lower than the first optimized system. From Table 9, two constraints are active for this optimized system, the rotation around the X axis in the second maneuvering condition, and the displacement in the X direction in the first maneuvering condition.

The second starting point had a very high axial stiffness of 20,000, and a radial stiffness of 100,000 lb/in. The second starting point and its corresponding optimum system are shown in Table 10. Also, from Table 11, it can be seen that the rotation of the engine c.g. in the X direction of the second maneuvering condition is the only active constraint. The interesting result here is that a very stiff mount can deliver equal performance to a very soft mount (by objective function comparison). One problem, however, with a stiffer mounting system is that the lumped parameter 6 degree-of-freedom mounting system model may no longer be valid. As the stiffness of the mounts increases, so does the natural frequency of the system, and wave effects become apparent due to the system behaving like a distributed system.

It can be seen from the three runs described above that the optimization technique is very reliable for this application. A solution was found for each starting point that successfully

Table 7 Deflection at the engine c.g.

	U_{tx}	U_{ty}	U_{tz}	U_{rx}	U_{ry}	U_{rz}
Static	−0.0084	0.0000	−0.0435	0.0000	−0.0429	0.0000
0.16 G in X	0.0055	0.0000	0.0013	0.0000	0.0129	0.0000
1000 in.-lb	0.0000	0.0039	0.0000	−0.0200	0.0000	0.0005

Table 8 Comparison between original and optimized systems (soft starting point)

	Original system	Optimized system
Objective function	0.030	0.093
K_X, Axial stiffness	4,000	10,650
K_Y and K_Z, Radial stiffness	2,000	2,418
Natural frequencies, Hz	5.10	6.58
	6.46	7.82
	7.94	9.18
	9.82	21.28
	13.63	25.24
	21.01	27.82

Table 9 Deflection at engine c.g. (soft starting point)

	U_{tx}	U_{ty}	U_{tz}	U_{rx}	U_{ry}	U_{rz}
Static	−0.0084	0.0000	−0.0435	0.0000	−0.0429	0.0000
0.16 G in X	0.0300	0.0000	0.0013	0.0000	0.0129	0.0000
1000 in.-lb	0.0000	0.0039	0.0000	−0.0200	0.0000	0.0005

Table 10 Comparison between original and optimized systems (stiff starting point)

	Original system	Optimized system
Objective function	0.153	0.093
K_X, Axial stiffness	20,000	10,568
K_Y and K_Z, Radial stiffness	100,000	114,680
Natural frequencies, Hz	14.32	10.58
	18.24	13.38
	25.81	18.92
	53.72	57.38
	65.14	68.71
	124.01	131.24

Table 11 Deflection at engine c.g. (stiff starting point)

	U_{tx}	U_{ty}	U_{tz}	U_{rx}	U_{ry}	U_{rz}
Static	−0.0084	0.0000	−0.0437	0.0000	−0.0428	0.0000
0.16 G in X	0.0031	0.0000	0.0013	0.0000	0.0129	0.0000
1000 in.-lb	0.0000	0.0039	0.0000	−0.0200	0.0000	0.0005

lowered the transmitted forces in the mounts, while satisfying the static deflection constraints. One problem yet to be solved, however, is that of locating a global minimum instead of the nearest local minima. In the hope of locating a global minimum, it is suggested that more than one starting point be tried.

For this numerical example, the two latter cases yielded a better solution. For the starting point with a low mount stiffness, the resulting optimum system had mounts with a low radial stiffness, and lower natural frequencies. For the starting point with a high mount stiffness, the optimum system had mounts with a high radial stiffness, and higher natural frequencies.

Conclusions

The simulation and numerical optimization of aircraft engine mounting systems are demonstrated using an interactive computer program called Sixopt. The rigid body engine is supported by elastomeric mounts on a rigid base. Vibratory forces transmitted through the elastomeric mounts under certain engine excitation conditions are minimized by adjusting the stiffness and orientation of the engine mounts. Inequality constraints on the maximum allowable deflection of the engine to static and maneuvering conditions must also be satisfied. The constrained variable metric optimization technique solves for the optimum design. The technique has been demonstrated successfully on an example.

Acknowledgments

The authors of this article express their appreciation to R. W. Mayne of SUNY at Buffalo for his assistance in implementing the computer program CVM01 in this work. They also thank P. T. Herbst for his advice and for supplying the photographs.

References

[1]Demic, M., "A Contribution to the Optimization of the Characteristics of Elastodamping Elements of Passenger Cars," *Vehicle System Dynamics*, Vol. 19, No. 1, 1990, pp. 3–18.

[2]Bernard, J. E., and Starkey, J. M., "Engine Mount Optimization," Society of Automotive Engineers Paper 830257, Feb. 1983.

[3]Spiekermann, C. E., Radcliffe, C. J., and Goodman, E. D., "Optimal Design and Simulation of Vibrational Isolation Systems," *Journal of Mechanisms, Transmissions, and Automation in Design*, Vol. 107, June 1985, pp. 271–276.

[4]Zhou, J., and Mayne, R. W., "Monotonicity Analysis and Recursive Quadratic Programming in Constrained Optimization," *Journal of Mechanisms, Transmissions, and Automation in Design*, Vol. 107, Oct. 1985, pp. 459–462.

[5]Haug, E. J., *Computer-Aided Kinematics and Dynamics of Mechanical Systems, Volume I: Basic Methods*, Allyn and Bacon, Needham Heights, MA, 1989.

[6]Powell, M. J. D., "A Fast Algorithm for Nonlinearly Constrained Optimization Calculations," *Numerical Analysis*, edited by G. A. Watson, Dundee, Scotland, 1977; see also *Lecture Notes in Mathematics No. 630*, Springer-Verlag, New York, 1978.